



Journal of The Ferrata Storti Foundation

The lifespan quantitative trait locus gene Securin controls hematopoietic progenitor cell function

by Andreas Brown, Desiree Schuetz, Yang Han, Deidre Daria, Kalpana J Nattamai, Karina Eiwen, Vadim Sakk, Johannes Pospiech, Thomas Saller, Gary van Zant, Wolfgang Wagner, and Hartmut Geiger

Haematologica 2019 [Epub ahead of print]

Citation: Andreas Brown, Desiree Schuetz, Yang Han, Deidre Daria, Kalpana J Nattamai, Karina Eiwen, Vadim Sakk, Johannes Pospiech, Thomas Saller, Gary van Zant, Wolfgang Wagner, and Hartmut Geiger. The lifespan quantitative trait locus gene Securin controls hematopoietic progenitor cell function.

Haematologica. 2019; 104:xxx

doi:10.3324/haematol.2018.213009

Publisher's Disclaimer.

E-publishing ahead of print is increasingly important for the rapid dissemination of science. Haematologica is, therefore, E-publishing PDF files of an early version of manuscripts that have completed a regular peer review and have been accepted for publication. E-publishing of this PDF file has been approved by the authors. After having E-published Ahead of Print, manuscripts will then undergo technical and English editing, typesetting, proof correction and be presented for the authors' final approval; the final version of the manuscript will then appear in print on a regular issue of the journal. All legal disclaimers that apply to the journal also pertain to this production process.

The lifespan quantitative trait locus gene *Securin* controls hematopoietic progenitor cell function

Andreas Brown¹, Desiree Schuetz¹, Yang Han², Deidre Daria³, Kalpana J. Nattamai³, Karina Eiwien¹, Vadim Sakk¹, Johannes Pospiech¹, Thomas Saller¹, Gary van Zant⁴, Wolfgang Wagner², and Hartmut Geiger^{1,3}

¹Institute of Molecular Medicine and Stem Cell Aging, Ulm University, Ulm, Germany

²Helmholtz-Institute for Biomedical Engineering, Stem Cell Biology and Cellular Engineering, RWTH Aachen University Medical School, Aachen, Germany

³Division of Experimental Hematology and Cancer Biology, Cincinnati Children's Hospital Medical Center and University of Cincinnati, Cincinnati, OH, USA

⁴University of Kentucky College of Medicine. UK Medical Center, Lexington, KY, USA

CONTACT:

Hartmut Geiger, Institute of Molecular Medicine and Stem Cell Aging, Ulm University, 89081 Ulm, Germany and Cincinnati Children's Hospital Medical Center, Cincinnati, OH 45229, USA.

Email: hartmut.geiger@uni-ulm.de

Phone: +1 513-636-1338 or +49 731 500 57650

Fax: +1 513-636-3768 or +49 731 500 57652

RUNNING TITLE: *Securin* controls hematopoietic progenitor function

WORD COUNT: 3,226; **MAIN FIGURES:** 4

Abstract

The percentage of murine hematopoietic stem and progenitor cells, which present with a loss of function upon treatment with the genotoxic agent hydroxyurea, is inversely correlated to the mean lifespan of inbred mice, including the long-lived C57BL/6 and short-lived DBA/2 strains. Quantitative trait locus mapping in BXD recombinant inbred strains identified a region spanning 12.5 cM on the proximal part of chromosome 11 linked to both the percentage of dysfunctional hematopoietic stem and progenitor cells as well as regulation of lifespan. By generating and analyzing reciprocal congenic mice for this locus, we demonstrate that this region indeed determines the sensitivity of hematopoietic stem and progenitor cells to hydroxyurea. These cells do not present, as previously anticipated, with differences in cell cycle distribution, and also not with changes in the frequency of cells undergoing apoptosis, senescence, replication stalling and re-initiation activity, excluding that variations in proliferation, replication or viability underlie the distinct response of these cells from the congenic and parental strains. An epigenetic aging clock in blood cells was accelerated in C57BL/6 mice congenic for the DBA/2 version of the locus. We verified pituitary tumor-transforming gene-1 (*Pttg1*)/*Securin* as the quantitative trait gene regulating the differential response of hematopoietic stem and progenitor cells to hydroxyurea treatment and which might thus likely be linked to the regulation of lifespan.

Introduction

We previously reported a correlation between the frequency of hematopoietic stem and progenitor cells (HSPCs) from a set of inbred mouse strains with impaired progenitor cell function upon treatment with hydroxyurea (HU) and the mean lifespan of these mice. The set of inbred strains also included C57BL/6 (B6) (low frequency of HSPCs dysfunctional in response to HU, long lifespan) and DBA/2 (D2) (high frequency of HSPCs dysfunctional in response to HU, short lifespan). In these experiments, the *in vitro* cobblestone area forming cell (CAFC) assay was used to determine the number of functional HSPCs before and after treatment with HU. Given that HU kills proliferating cells via the induction of DNA strand breaks that arise from stalled replication forks after depletion of the nucleotide pool, this finding was interpreted as a significantly higher percentage of HSPCs from D2 versus B6 in S-phase and subsequently that elevated levels of HSPC proliferation could be negatively linked to lifespan.¹⁻³ Using BXD recombinant inbred (RI) mice, which are genetic chimeras based on B6 and D2, subsequently a quantitative trait locus (QTL) was mapped to chromosome 11 linked to the frequency of HSPCs susceptible to HU. Interestingly, the same locus showed also a linkage to the mean lifespan within the BXD RI set of mice, transforming the reported phenotypic correlation into a genetic connection, implying a common underlying gene and thus mechanism for the regulation of both phenotypes. To verify the linkage and identify the underlying quantitative trait gene, we generated B6 as well as D2 mice that are reciprocally congenic for this locus on chromosome 11.

Methods

Mice

Laboratory C57BL/6J (B6), DBA/2J (D2) and BXD inbred mice were obtained from Janvier Labs (France). All mice were fed acidified water and food *ad libitum*, and housed under pathogen-free conditions at the University of Kentucky, Division of Laboratory Animal Resource and the Animal Facility of Ulm University. Mouse experiments were performed in compliance with the German Law for Welfare of Laboratory Animals and were approved by the Regierungspräsidium Tübingen.

QTL mapping

Linkage analysis and determination of the likelihood ratio statistic values for suggestive linkage were performed as described by using WebQTL (<http://www.genenetwork.org/webqtl/main.py?FormID=submitSingleTrait>), identifying the restrictive chromosome 11 locus, among others, correlating to mean life span and HU sensitivity.³⁻⁶

Generation of congenic mice

Congenic animals were generated in five generations by a marker-assisted backcrossing strategy as described (^{3,5,7-9} and **Fig 1C**). The particular DBA/2J genomic region was derived from BXD31, one of the BXD recombinant inbred strains used in the QTL mapping and which phenotypically best demonstrated the decline in HSCs in old age and the HU-sensitivity.³

Preparation of hematopoietic tissue and cells

For the isolation of total BM, *tibiae*, *femur* and hips of mice were isolated and flushed using a syringe and a G21 needle. Mononuclear (low density bone marrow, LDBM) cells were isolated by Histopaque low-density centrifugation (#10831, Sigma). Lineage depletion was performed using the mouse lineage cell depletion Kit (#130-090-858, Miltenyi Biotec) according to their protocol.

CAFC Assay

CAFC assay was performed as described.¹ Briefly, 1,000 FBMD-1 cells, a stromal cell line, were seeded in each well of 96-well plates. Plates were incubated at 33 °C in 5% CO₂, and used 7 days later for CAFC assay. Bone marrow cells were either treated with 200 µg/ml HU or its solvent (PBS) and seeded onto the pre-established stromal layers in six dilutions, serially in threefold increments from 333 to up to 81,000 cells/well (12 wells per dilution). At this time, the medium was switched from 5% horse serum and 10% fetal bovine serum to 20% horse serum. Alternatively, mice were treated with HU *in vivo* as indicated following bone marrow isolation and seeding. After 7 days, all wells were evaluated for the presence or absence of cobblestone areas and the frequency of the appearance of a colony calculated using L-Calc software (STEMCELL Technologies).

Analysis of the epigenetic aging signature

Analysis of DNA methylation levels was analyzed at three age-associated CG dinucleotides (CpGs) as described previously.¹⁰ Briefly, genomic DNA was isolated from blood samples, bisulfite converted, and DNA methylation was analyzed within the three genes (*Primal*, *Hsf4*, *Kcns1*) by pyrosequencing. The DNA methylation results at these sites can be integrated into a multivariable model for epigenetic age predictions in B6 mice, which clearly correlate with the chronological age.¹⁰

Statistical Analysis

All statistical analyses were performed using Student's t-test or 2-way Anova, when appropriate with GraphPad Prism 6 software. For *Fig 4C* linear and non-linear regression was calculated. The number of biological repeats (n) is indicated in figure legends. Error bars are SEM.

Results

HSPCs from BXD RI strains show highly divergent reactions when exposed to HU as judged by their ability to form cobblestones on stromal feeder layers in the CAFC assay after 7 days of culture (CAFC day 7 assay).⁹ Re-analyzing the initial phenotypic data based on the most recent marker map (New Genotypes 2017 dataset) provided for BXD RI strains, verified the initially identified locus on chromosome 11 (35-75 Mb) linked (with a suggestive threshold of 10.53/10.88) to both HU susceptibility of HSPCs as well as mean lifespan of the analyzed mice (*Figs 1A+B, Suppl Tables 1A+B*,³). We used a marker assisted speed congenic approach to obtain a reciprocal set of mice congenic for the chromosome 11 locus (*Fig 1C*). These novel mouse lines were named line A (D2 onto B6) and K (B6 onto D2). We performed whole genome SNP mapping of our congenic mouse strains to identify the length of the congenic intervals transferred as well as the overlap between the reciprocal strains. Ultimately, the common region transferred in line A and line K spans an 18.6 Mb (8.3 cM) region on chromosome 11 from rs26900200, 37,929,686 bp to rs3088940, 56,516,067 bp with no other transferred intervals stemming from the donor strains that are identical between the two congenic strains. The SNP analysis further revealed a small set of additional congenic regions in both line A and K animals, though not covering identical regions (*Fig 1D, Suppl Fig 1, Suppl Table 2*). This interval contains about 130 protein coding genes (*Suppl Table 3*).

We next tested, based on the CAFC assay, whether the genotype of the locus conferred in the congenic strains correlated with the magnitude of our phenotype of HSPCs susceptible to HU. HU treatment efficiently suppresses BrdU incorporation and thus active S-Phase in freshly isolated Lin-cKit⁺ (LK) cells from all strains (*Suppl. Fig 2A*). Indeed, HSPCs isolated from B6 or line K (B6 onto D2) mice presented with a lower frequency of dysfunctional HSPCs in response to short term *in vivo* as well as to *ex vivo* treatment with

HU, while inversely, D2 and line A (D2 onto B6) HSPCs were more sensitive to HU (**Fig 2A, Suppl Fig 2B**). These data confirm that the interval on chromosome 11 shared among the congenic strains confers this phenotype and might thus contain a gene regulating the response of HSPCs to HU.

Since HU inhibits dNTP synthesis,¹¹ and a lack of dNTPs causes replication fork stalling and thus DNA damage and apoptosis,¹² it is believed that the frequency of cells susceptible to HU treatment is an indirect measurement for the frequency of cells in the S-phase of the cell division cycle. It has been thus concluded that the underlying mechanism of the distinct susceptibility of HSPCs from the inbred strains is due to distinct S-phase frequencies. BM cells with the Lin-cKit⁺ surface marker combination (hematopoietic progenitor cells, LK cells) are highly enriched for CAFC day 7 cells (**Suppl Fig 2C**). Analysis of the frequency of LK cells from the inbred and the congenic strains in different stages of the cell division cycle by *in vivo* BrdU incorporation and flow cytometry, as well as that of hematopoietic stem cells (HSCs) and less primitive progenitors (LSKs), however, revealed almost identical patterns and especially almost identical frequencies of cells in S-phase among all the strains tested (**Fig 2B**). HU susceptibility in HSPCs does therefore not correlate with the frequency of HSPCs in S-phase, which excludes differences in cycling frequencies as the underlying mechanism for the phenotype observed, as well as in general HU susceptibility as surrogate for the frequency of cells in S-phase. Consistent with that finding was the fact that HSPCs from all groups had similar telomere lengths. Short telomeres can be seen as a surrogate marker for high levels of proliferation (**Suppl Fig 2D**). In addition, the frequency of LKs and LSKs was very similar in all strains, while D2-derived mice displaying a general higher HSC frequency, as already reported,¹ which is, however, not mirrored in B6/line A mice and thus locus-independent. That finding excludes a difference in the number of these cells as a factor contributing to the phenotype (**Fig 2C**). Furthermore, the frequencies of HSPCs undergoing

apoptosis upon *ex vivo* HU treatment and under steady state conditions *in vivo* were at a low level among these groups, even when regarding S-phase specific apoptosis rates as well senescence in response to HU as indicated by the level of the senescence marker *p16* in HSPCs (**Fig 2D**, **Suppl Figs 2E,F**). In addition, whereas HU treatment almost completely blocks BrdU incorporation, LK cells from all strains preserve their ability to re-enter active S-phase in a locus-independent manner 3 and even 16 h after HU is removed, excluding that enhanced levels of senescence, apoptosis or difference in re-initiation of replication after stalling are causative for the HU sensitivity phenotype (**Fig 2E**, **Suppl Fig 2G**). Similarly, LK cells from all strains showed comparable frequencies of γ H2AX foci per cells upon HU treatment and 3 h post HU removal, which also excludes a role of variation in stalling of replication and the subsequent DNA damage for our phenotype (**Fig 2F**). In aggregation, these data exclude a likely contribution of differences in cell cycle and replication parameters as well as differential senescence or apoptosis to the highly unequal HU susceptibilities of HSPCs in the inbred and congenic strains, while the underlying mechanism still remains to be identified.

A D2-allele at the genetic microsatellite marker *D11Mit174* (Chr.11:42,593,949-42,594,095, which is within the area with the highest level of linkage) correlated in the BXD RI set, as anticipated, with higher HU-susceptibility rates of HSPCs and a lower mean life span (**Fig 3A**). The gene *Pttg1* (*Securin*), which has been reported to inhibit mitotic division^{13,14} is located in very close proximity (+ 800 kB) to *D11Mit174*.¹⁵ In addition, the yeast homolog of *Securin*, *Pds1p*, was reported to be critically involved in the regulation of the intra-S-checkpoint and regulation of the response of yeast to treatment with HU.¹⁶ Previously, a 3-11-fold overexpression of *Pttg1* in various D2 tissues compared to B6 was demonstrated.¹⁷⁻¹⁹ This renders *Pttg1* a prime candidate quantitative trait gene in the interval on chromosome 11. To investigate whether the *Pttg1* mediates the HU response, we analyzed its expression in

our experimental mouse strains: We observed a 3-5 fold increase in gene and protein expression in D2 or line A derived HSPCs compared to the corresponding cells from B6 or line K mice (**Figs 3B,C**). A D2-allele of the locus thus confers elevated expression of *Pttg1*. Analyzing *Pttg1*-associated promoter and exon regions *in silico* revealed a 7 bp insertion downstream of the transcription start (NCBI Reference Sequence: NC_000077.6) in the D2 genome, potentially positively affecting binding of transcription factors (TF) (**Suppl Fig 3A**). Since the occurrence of these D2- and A/J-specific 7 bp was previously reported to result in reduced *Pttg1* expression in contrast to what we find in D2 animals,²⁰ we further determined the promoter structure of *Pttg1* in more detail by PCR of genomic DNA. Surprisingly, the *Pttg1* promoter region was present in two differently sized versions (the two fragments differ in size by approx. 700 bp) in D2 and line A mice (**Fig 3D**). DNA sequencing revealed that the short version in D2 (D2_1) was identical to the B6 *Pttg1* promoter, while the longer version (D2_2) was unique to D2 and included the already described 7 bp insertion in addition to an additional 675 bp region between the transcription and the ORF start, which is not completely annotated in common genome databases at present time in contrast to the 7 bp insertion (**Suppl Figs 3B,C**). This could imply a likely gene duplication of *Pttg1* within the congenic locus. We next tested whether the distinct types of promoter regions are causative for the dissimilar *Pttg1* expression patterns. By applying a dual-specific luciferase assay, we observed an almost three-fold increase in activity of the D2_2-specific promoter compared to the B6 and the shorter D2_1 variants, suggesting that not the 7 bp insertion but the additional 675 bp region drive elevated levels of *Pttg1* expression in D2 or A cells (**Fig 3E**). We also identified several exon-specific SNPs causing amino acid substitutions in *Pttg1*. Using 3D *in silico* models that predict the protein structure of PTTG1, no obvious difference in the structure was observed between the B6 and D2 variants besides a slight increase in 3₁₀ helices, a common secondary structure, which renders an additional contribution of the coding SNPs of *Pttg1* to the phenotype less likely (**Suppl Fig 4A**).

To test whether *Pttg1* is indeed the QTL gene within the described locus and thus whether the increased HU-sensitivity of HSPCs is caused by elevated *Pttg1* levels we overexpressed a *Pttg1-Egfp* fusion gene by lentiviral transduction in B6 HSPCs. The level of expression of the transgene was within the range of the difference in gene expression between B6 and D2 HSPCs and thus in a physiological range (**Fig 4A, left panel**). Transduced bone marrow cells were transplanted into B6 recipients for their *in vivo* expansion. We sorted GFP+ BM cells 5 weeks post transplantation to analyze the susceptibility of HSPCs to HU with the CAFC assay. BM cells of the transplanted mice were presented with similar rates of transduction (GFP+ cells), excluding a potential bias of certain subpopulations upon transduction (**Suppl. Figs 4B,C**). Elevated expression of *Pttg1* in B6 HSPCs resulted in a significant increase in their susceptibility to HU treatment (**Fig 4A, right panel**). Similarly, upon downregulation of *Pttg1* in progenitor cells from line A and D2 mice, we observed a trend towards reduced HU sensitivity (**Suppl Fig 4D**). These data confirm a causative role for distinct levels of expression of *Pttg1* for the susceptibility of HSPCs to short term HU treatment, and thus strongly imply that *Pttg1* is the QTL gene within the QTL locus.

Ultimately, the question remains whether the locus also accounts for a variation in life span. Previously, the methylation status of CpG sites within the genes *Prima1*, *Hsf4*, *Kcns1* was shown to qualify as a reliable predictor of chronological age of B6 mice.¹⁰ This same study also revealed enhanced epigenetic aging of the D2 strain in accordance with its general reduced mean life span, supporting the possibility that the panel might also serve as a marker for the biological age in mice. Applying this B6-trained marker panel to our (congenic) experimental strains, we observed that epigenetic age predictions correlated with chronological age in B6 ($R^2 = 0.93$) and line A mice ($R^2 = 0.89$). Notably, epigenetic aging was clearly accelerated in line A mice compared to B6 (**Figs 4B+C**). We have previously

demonstrated that in D2 mice the same epigenetic age predictor significantly accelerated epigenetic age predictions that rather follow a logarithmic regression¹⁰, which line K though did not deviate from (*Figs 4B+C*). More in depth analyses for line K would warrant the development of an improved age predictor that is adjusted to more control samples of D2, as the initial marker panel was trained on B6. The data are though consistent with a possible role of the QTL in affecting lifespan at least of line A mice, which will need to be ultimately tested in longevity studies of larger cohorts of animals.

Discussion

Forward genetic approaches in BXD RI strains have been proven to allow for the identification of QTLs linked to lifespan and changes in various tissues and cells upon aging.^{22,23} We previously reported the likely linkage of a locus on the distal part of murine chromosome 11 to two phenotypes, regulation of lifespan as well the susceptibility of HSPCs to short term treatment with HU. While this finding implies a common mechanism of regulation for the two phenotypes, speculations on the mechanistic connection between these two phenotypes remains difficult without the identification of the gene within the locus regulating at least one of the phenotypes. Here, by generating and analyzing reciprocal strains congenic for the interval on chromosome 11 (B6 onto D2 and D2 onto B6), we verify the initial linkage analysis by demonstrating that this locus indeed controls the susceptibility of HSPCs to HU. Other loci than the chromosome 11 locus may at least in part also contribute to the HU response phenotype, as line A and K mice are also congenic for other loci in addition to the locus on chromosome 11 (*Suppl. Fig.1*). The proximal locus on chromosome 11, which spans about 18.6 Mb, is however the only region which is identical between both congenic mouse strains, making a substantial contribution of other loci less likely (*Suppl. Table 2*). Unexpectedly, elevated sensitivity of HSPCs to HU is not linked to altered cell cycle activity and thus elevated numbers of HSPCs in S-phase, nor to apoptosis, senescence or enhanced replication fork stalling as might be anticipated by previously reported outcomes to HU exposure. The precise mechanism that confers elevated susceptibility thus still remains to be further investigated. Our data strongly support *Pttg1/Securin* to be the QTL gene in that interval, as elevated levels of its expression conferred by the D2 allele result in increased HU susceptibility of HSPCs. Recently, *Pttg1* overexpression was reported to restrict BrdU incorporation and cause enhanced levels of senescence and DNA damage in proliferating human fibroblasts,²⁴ a feature which is not mirrored in HSPCs according to our data. Thus, these mechanistic differences illustrate the unique properties of HSPCs with respect to cell

cycle regulation and DNA damage response, as also demonstrated recently.²⁵⁻²⁷ The initial linkage data also imply a role for *Pttg1* in regulating lifespan. The primary role of *Pttg1* is an inhibition of Separase. This cysteine protease opens cohesin rings to allow for transition from metaphase to anaphase.²⁸ *Pttg1* is thus seen primarily as a target of the anaphase promoting complex (APC/C) to initiate chromosome segregation, although other additional roles have been described in the literature, like a central role in pituitary tumor formation when overexpressed.²⁹ Interestingly, the APC/C is directly involved in regulating lifespan in yeast and results in dysregulation of rDNA biology,³⁰ while likely dominant negative mutations in cohesin genes have been recently identified as novel contributors to the initiation of acute myeloid leukemia through modulation of chromatin accessibility in HSPCs and subsequent inhibition of differentiation by recruiting “stemness” transcription factors to the daughter cells upon division. Extended presence of cohesin, in the case of elevated levels of *Pttg1*, might thus contribute to loss of HSPC potential, which would be consistent with our phenotype (*Suppl Fig 4B*). Hence, the two phenotypes might be mechanistically connected via alterations in the epigenetic landscape rather than changes in chromatid cohesion itself. This interpretation is supported by the finding that age-associated DNA methylation changes are acquired at different pace in congenic mouse strains. It is thus possible that HU treatment interferes with epigenetic parameters regulated by *Pttg1/Securin*.

Foot notes

Supplementary data

Supplementary data contains supplementary experimental procedures, supplementary references, four supplementary figures and three tables.

Acknowledgments

We thank the FACS core at Ulm University, especially Ali Gawanbacht-Ramhormose and Sarah Warth for cell sorting and the Central Animal Facility of Ulm University as well as the Comprehensive Mouse and Cancer Core at CCHMC for help with mouse experiments. We are grateful to José Cancelas for providing us FBMD-1 stromal feeder cells. We thank Karin Müller from the Internal Medicine III Department for assistance with the GloMax 96 luminometer, Sebastian Iben from the Dermatology Department for helpful advice regarding the promotor studies and all lab members for fruitful discussions.

Author contributions

DS conducted some of the experiments with essential support from AB, KE and TS; HG and AB designed most of the experiments; YH and WW performed CpG analysis of the age-predictor genes, DD, KJN, GZ and HG were involved in analyzing BXD strains and generating the congenic mice; VS performed transplantation of transduced cells into B6 recipients and assisted with mouse crossings and maintenance of the congenic mouse cohort; JP generated the 3D models of PTTG1 and established protocols for the luciferase assay; AB and HG wrote the manuscript.

Grant support

Work in the laboratory of HG is supported by the Deutsche Forschungsgemeinschaft SFB 1074 and the RTG 1789, the Edward P. Evans Foundation and the National Institute of Health, AG040118, DK104814 and AG05065. AB was supported by a Bausteinprogramm of the Medical Faculty of Ulm University. WW was supported by the Else Kröner-Fresenius-Stiftung (2014_A193); by the Interdisciplinary Center for Clinical Research within the faculty of Medicine at the RWTH Aachen University (O3-3); by the Deutsche Forschungsgemeinschaft (WA 1706/8-1 and WA1706/11 1), and by Deutsche Krebshilfe (TRACK-AML).

Conflict of interests:

WW is involved in Cygenia GmbH (www.cygenia.com), which provides services for epigenetic age predictions. Apart from this the authors declare that there is no conflict of interests regarding the publication of this paper.

References

1. De Haan G, Nijhof W, Van zant G. Mouse strain-dependent changes in frequency and proliferation of hematopoietic stem cells during aging: correlation between lifespan and cycling activity. *Blood*. 1997;89(5):1543-1550.
2. Lopes M, Cotta-ramusino C, Pellicoli A, et al. The DNA replication checkpoint response stabilizes stalled replication forks. *Nature*. 2001;412(6846):557-561.
3. De Haan G, Bystrykh LV, Weersing E, et al. A genetic and genomic analysis identifies a cluster of genes associated with hematopoietic cell turnover. *Blood*. 2002;100(6):2056-2062.
4. Geiger H, Rennebeck G, Van zant G. Regulation of hematopoietic stem cell aging in vivo by a distinct genetic element. *Proc Natl Acad Sci USA*. 2005;102(14):5102-5107.
5. Geiger H, True JM, De haan G, Van zant G. Age- and stage-specific regulation patterns in the hematopoietic stem cell hierarchy. *Blood*. 2001;98(10):2966-2972.
6. Manly KF, Cudmore RH, Meer JM. Map Manager QTX, cross-platform software for genetic mapping. *Mamm Genome*. 2001;12(12):930-932.
7. Van Zant G, Holland BP, Eldridge PW, Chen JJ. Genotype-restricted growth and aging patterns in hematopoietic stem cell populations of allophenic mice. *J Exp Med*. 1990;171(5):1547-1565.
8. Wakeland E, Morel L, Achey K, Yui M, Longmate J. Speed congenics: a classic technique in the fast lane (relatively speaking). *Immunol Today*. 1997;18(10):472-477.

9. De Haan G, Van zant G. Dynamic changes in mouse hematopoietic stem cell numbers during aging. *Blood*. 1999;93(10):3294-3301.
10. Han Y, Eipel M, Franzen J, et al. Epigenetic age-predictor for mice based on three CpG sites. *Elife*. 2018;7.
11. Young CW, Schochetman G, Karnofsky DA. Hydroxyurea-induced inhibition of deoxyribonucleotide synthesis: studies in intact cells. *Cancer Res*. 1967;27(3):526-534.
12. Koç A, Wheeler LJ, Mathews CK, Merrill GF. Hydroxyurea arrests DNA replication by a mechanism that preserves basal dNTP pools. *J Biol Chem*. 2004;279(1):223-230.
13. Funabiki H, Kumada K, Yanagida M. Fission yeast Cut1 and Cut2 are essential for sister chromatid separation, concentrate along the metaphase spindle and form large complexes. *EMBO J*. 1996;15(23):6617-6628.
14. Funabiki H, Yamano H, Kumada K, Nagao K, Hunt T, Yanagida M. Cut2 proteolysis required for sister-chromatid separation in fission yeast. *Nature*. 1996;381(6581):438-441.
15. Hood HM, Metten P, Crabbe JC, Buck KJ. Fine mapping of a sedative-hypnotic drug withdrawal locus on mouse chromosome 11. *Genes Brain Behav*. 2006;5(1):1-10.
16. Schollaert KL, Poisson JM, Searle JS, Schwanekamp JA, Tomlinson CR, Sanchez Y. A role for *Saccharomyces cerevisiae* Chk1p in the response to replication blocks. *Mol Biol Cell*. 2004;15(9):4051-4063.

17. Bottomly D, Walter NA, Hunter JE, et al. Evaluating gene expression in C57BL/6J and DBA/2J mouse striatum using RNA-Seq and microarrays. *PLoS One*. 2011;6(3):e17820.
18. Geisert EE, Lu L, Freeman-anderson NE, et al. Gene expression in the mouse eye: an online resource for genetics using 103 strains of mice. *Mol Vis*. 2009;15:1730-1763.
19. Freeman NE, Templeton JP, Orr WE, Lu L, Williams RW, Geisert EE. Genetic networks in the mouse retina: growth associated protein 43 and phosphatase tensin homolog network. *Mol Vis*. 2011;17:1355-1372.
20. Keeley PW, Zhou C, Lu L, Williams RW, Melmed S, Reese BE. Pituitary tumor-transforming gene 1 regulates the patterning of retinal mosaics. *Proc Natl Acad Sci USA*. 2014;111(25):9295-9300.
21. Vadnais C, Davoudi S, Afshin M, et al. CUX1 transcription factor is required for optimal ATM/ATR-mediated responses to DNA damage. *Nucleic Acids Res*. 2012;40(10):4483-4495.
22. Lang DH, Gerhard GS, Griffith JW, et al. Quantitative trait loci (QTL) analysis of longevity in C57BL/6J by DBA/2J (BXD) recombinant inbred mice. *Aging Clin Exp Res*. 2010;22(1):8-19.
23. Henckaerts E, Langer JC, Snoeck HW. Quantitative genetic variation in the hematopoietic stem cell and progenitor cell compartment and in lifespan are closely linked at multiple loci in BXD recombinant inbred mice. *Blood*. 2004;104(2):374-379.

24. Hsu YH, Liao LJ, Yu CH, et al. Overexpression of the pituitary tumor transforming gene induces p53-dependent senescence through activating DNA damage response pathway in normal human fibroblasts. *J Biol Chem.* 2010;285(29):22630-22638.
25. Moehrle BM, Nattamai K, Brown A, et al. Stem Cell-Specific Mechanisms Ensure Genomic Fidelity within HSCs and upon Aging of HSCs. *Cell Rep.* 2015;13(11):2412-2424.
26. Brown A, Pospiech J, Eiwen K, et al. The Spindle Assembly Checkpoint Is Required for Hematopoietic Progenitor Cell Engraftment. *Stem Cell Reports.* 2017;9(5):1359-1368.
27. Brown A, Geiger H. Chromosome integrity checkpoints in stem and progenitor cells: transitions upon differentiation, pathogenesis, and aging. *Cell Mol Life Sci.* 2018;75(20):3771-3779.
28. Luo S, Tong L. Structural biology of the separase-securin complex with crucial roles in chromosome segregation. *Curr Opin Struct Biol.* 2018;49:114-122.
29. Sapochnik M, Nieto LE, Fuertes M, Arzt E. Molecular Mechanisms Underlying Pituitary Pathogenesis. *Biochem Genet.* 2016;54(2):107-119.
30. Sun D, Luo M, Jeong M, et al. Epigenomic profiling of young and aged HSCs reveals concerted changes during aging that reinforce self-renewal. *Cell Stem Cell.* 2014;14(5):673-688.

Figure legends

Figure 1: QTL analysis of HU responses and mean life spans of BXD mice and generation of mice congenic for the corresponding chromosome 11 locus

(A) WebQTL analysis of HU sensitivity rates and mean life spans of HSPCs isolated from various BXD and parental strains, identifying a proximal part of chromosome 11, among others, involved in this phenotype. Values are in *Likelihood Ratio Statistics* (LRS). (B) QTL analysis of mean life spans and HU responses of the various BXD strains for chromosome 11. (C) Schematic illustration showing the generation of the congenic mouse strains line A and K. Briefly, after crossing B6 with D2 mice, F1 littermates were backcrossed with the corresponding parental strains (B6/D2). Offspring was backcrossed in four rounds with parental strains reciprocal for the corresponding chromosome 11 specific SNP *D11Mit20* to finally obtain B6 or D2 mice congenic for the proximal locus on chromosome 11 of D2 or B6, respectively. (D) SNP analysis of chromosome 11 from strains B6, D2, A and K. HSPCs = Hematopoietic stem and progenitor cells, HU = Hydroxyurea, QTL = Quantitative trait locus

Figure 2: The chromosome 11 locus controls sensitivity of HSPCs to HU exposure but not HSPC frequency, cell cycle activity, apoptosis and replication fork stalling.

(A) Mice from all four groups were injected with 10 mg HU/kg body weight or its solvent (PBS) for 1 h following isolation of BM cells and processing for the CAFC assay. Shown is the fraction of HSPCs sensitive to HU. n=5-12. (B) Cell cycle distributions of HSCs (left panel), LSKs (middle panel) and LKs (right panel) of BrdU-treated mice. n=4. (C) Relative LDBM frequencies per *tibia* and *femur* of LKs, LSKs and HSCs of the four mouse strains. n=4. (D) Left panels: LDBM cells from the 4 strains were treated with HU or its solvent (PBS) for 1 h. Thereafter, LK cells (left panel) and HSCs (right panel) were analyzed in

terms of apoptosis (AnnexinV). n=4. (E) LDBM cells were either treated with a control (-HU), HU for 1 h or accordingly following HU removal by washing twice with medium and an additional resting period of 3 h (+HU Removal). 30 m prior to staining, all samples were co-cultured with BrdU. Left panel: Representative BrdU/7AAD FACS plots of LK cells from the indicated strains. Right panel: Quantification of LK cell cycle distribution. n=3. (F) LK cells from all four mouse strains were either treated with a control, HU for 1 h or accordingly following HU removal and an additional resting period of 3 h (+HU Removal). Thereafter, cells were harvested and stained against γ H2AX. Left panels: Representative confocal images. Right panel: Quantification of the number of γ H2AX foci per cell. n=3. Significances are related to the corresponding -HU controls. *P<0.05; **P<0.01; ***P<0.001; ****P<0.0001. HU = Hydroxyurea, HSPCs = Hematopoietic stem and progenitor cells, HSCs = Hematopoietic stem cells, LKs = Lin-cKit⁺ cells, LSKs = Lin-Sca1+cKit⁺ cells, LDBM = Low density bone marrow cells, RV = Removal

Figure 3: Chromosome 11 associated *Pttg1* has an altered promotor sequence in D2/A mice leading to enhanced expression

(A) Mean life span (left panel) or HU sensitivity rates of HSPCs (right panel) of BXD mouse strains relative to the occurrence of the SNP *D11Mit174*. (B) *Pttg1* gene expression in HSPCs from the indicated mouse strains. n=3. (C) PTTG1 protein expression in HSPCs from the four mouse strains. Left panel: Representative western blot images. Right panel: Quantification. n=3. (D) PCR analysis of genomic DNA from lines B6, D2, A and K using the primers 5'NheI-B6/D2_PTTG1_pr1 and 3'EcoRV-B6/D2_PTTG1_pr2. Major bands corresponding to the different promoters are indicated with arrows. (E) Dual-specific luciferase assay for the indicated promotor constructs, including a negative (pNL1.1[Nuc]) and a positive (pNL1.1[CMV]) control. The corresponding constructs illustrated from *Figure*

3D are highlighted in blue. n=3 (3 rounds with triplicates). *P<0.05; **P<0.01; ***P<0.0001. HU = Hydroxyurea, HSPCs = Hematopoietic stem and progenitor cells

Figure 4: *Pttg1* promotes HU sensitivity of HSPCs and influences epigenetic aging

(A) HSPCs from B6 mice were cytokine-stimulated and transduced with lentiviruses mediating stable endogenous *Pttg1-Egfp* (PTTG1 OE) or *Egfp* (control) overexpression. After transplantation into B6 recipients, total BM GFP+ cells were isolated, treated with HU or its solvent and processed for the CAFC assay. Left panel: RT-PCR analysis of transduced (GFP+) HSPCs. Right upper panel: Representative pictures of transduced day 7 cobblestones. Right bottom panel: Quantification of the frequency of HU-sensitive CAFs. n=3. (B+C) Epigenetic age predictions were determined based on DNA methylation at three CpG sites (*Prima1*, *Hsf4*, *Kcns1*). For B6 mice they followed a linear regression curve, whereas for D2 it followed a logarithmic trend, as described before.¹⁰ The deviance is the difference of the calculated age and the “real” chronological age of the four mouse strains. Mice per group: 26-40. (B) Regression curves and (C) dot plots of the corresponding methylation analyses. *P<0.05; ***P<0.001. HU = Hydroxyurea, HSPCs = Hematopoietic stem and progenitor cells, PH = Phase contrast

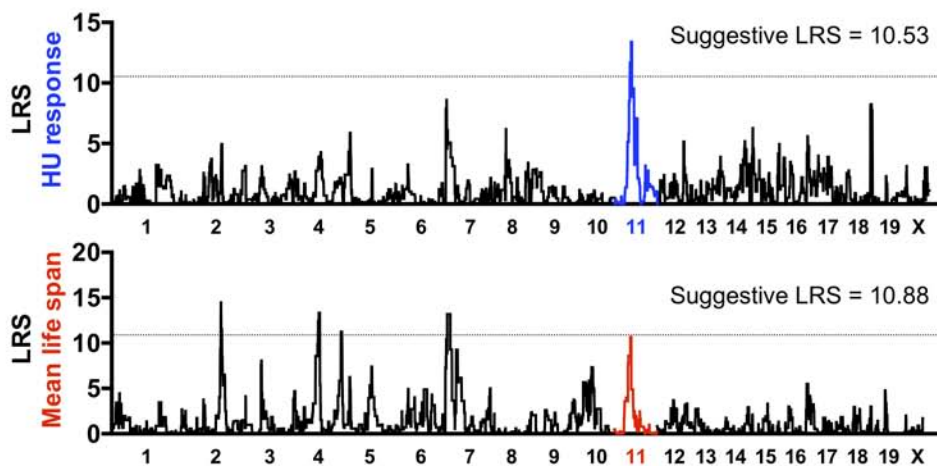
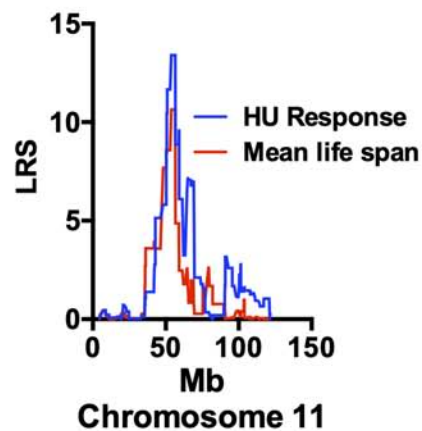
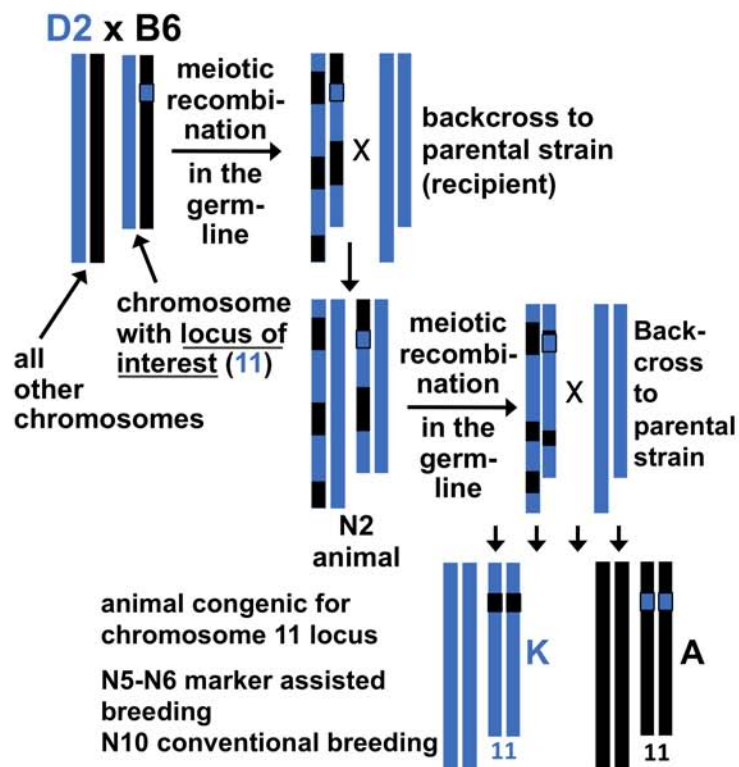
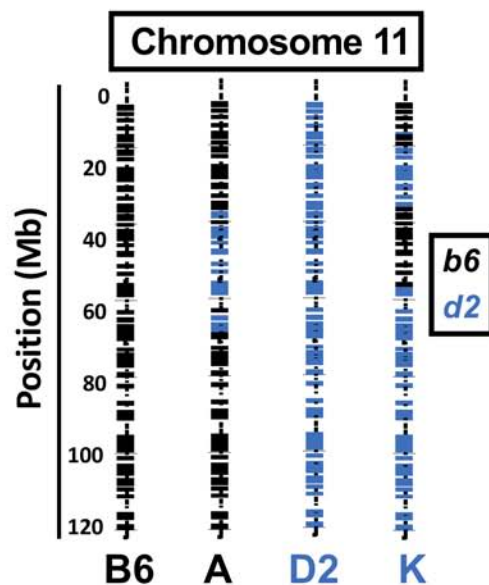
Fig 1**A****B****C****D**

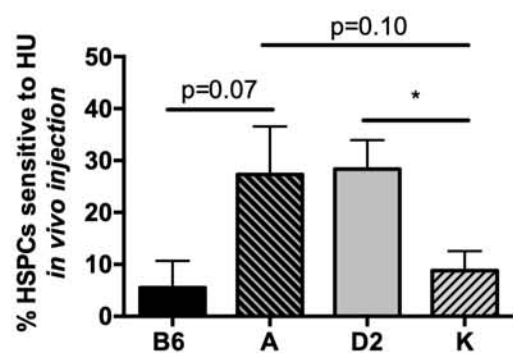
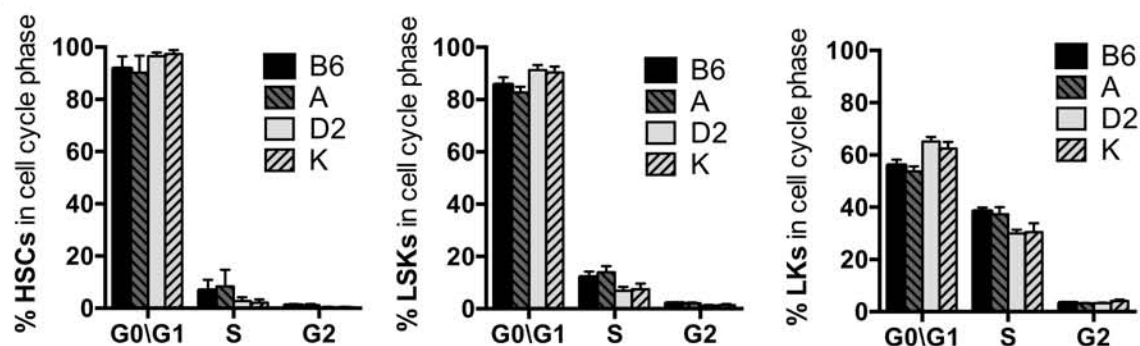
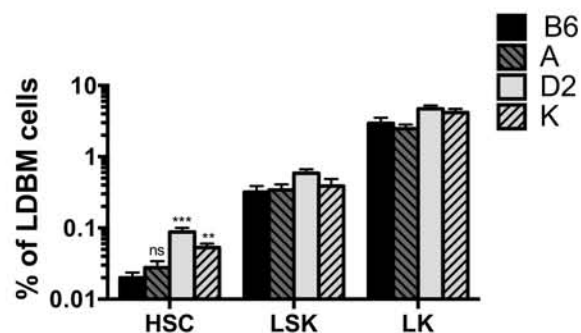
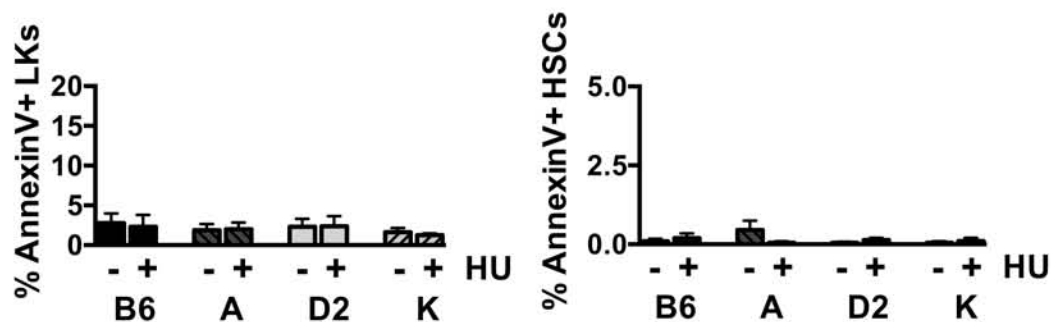
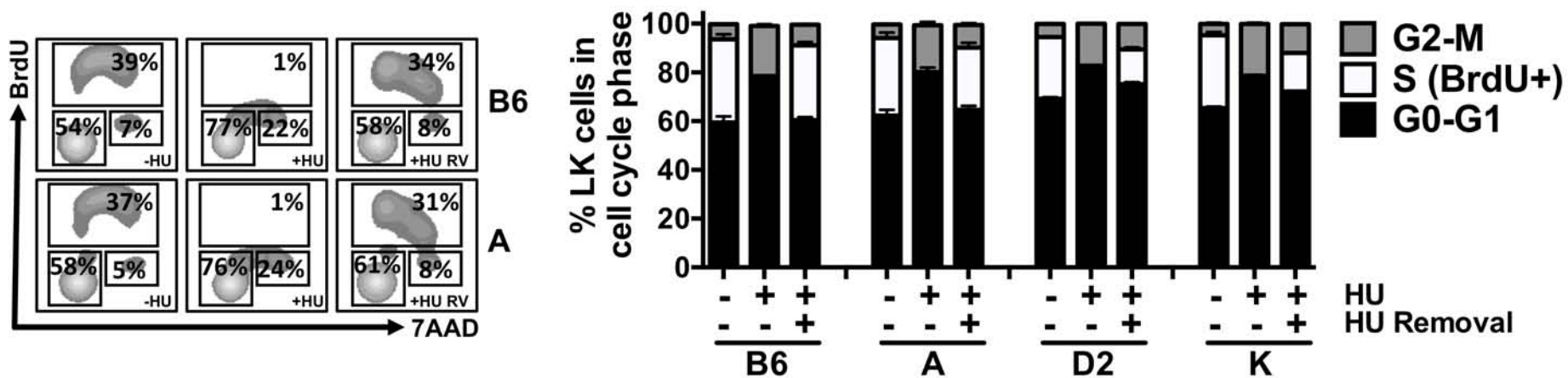
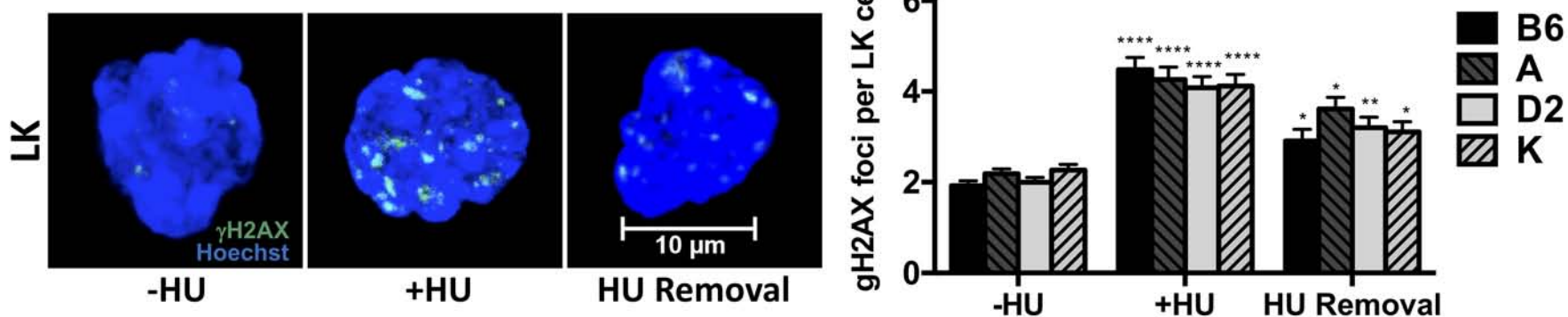
Fig 2**A****B****C****D****E****F**

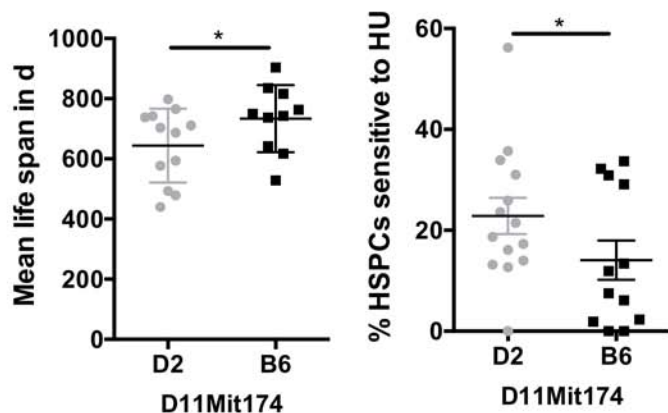
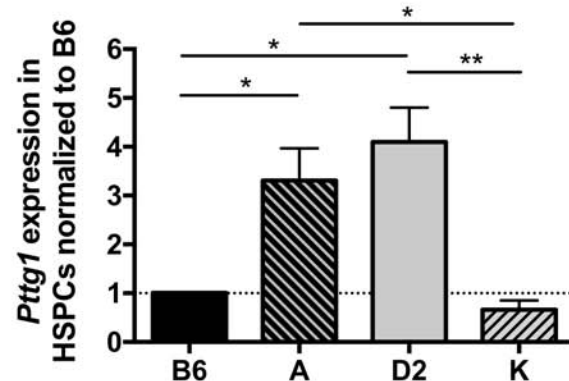
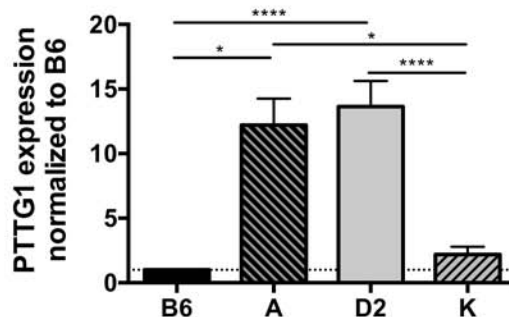
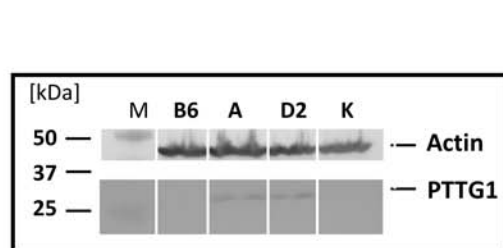
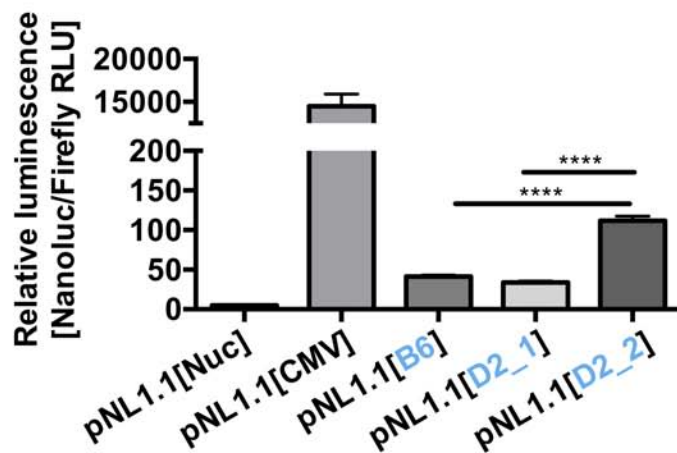
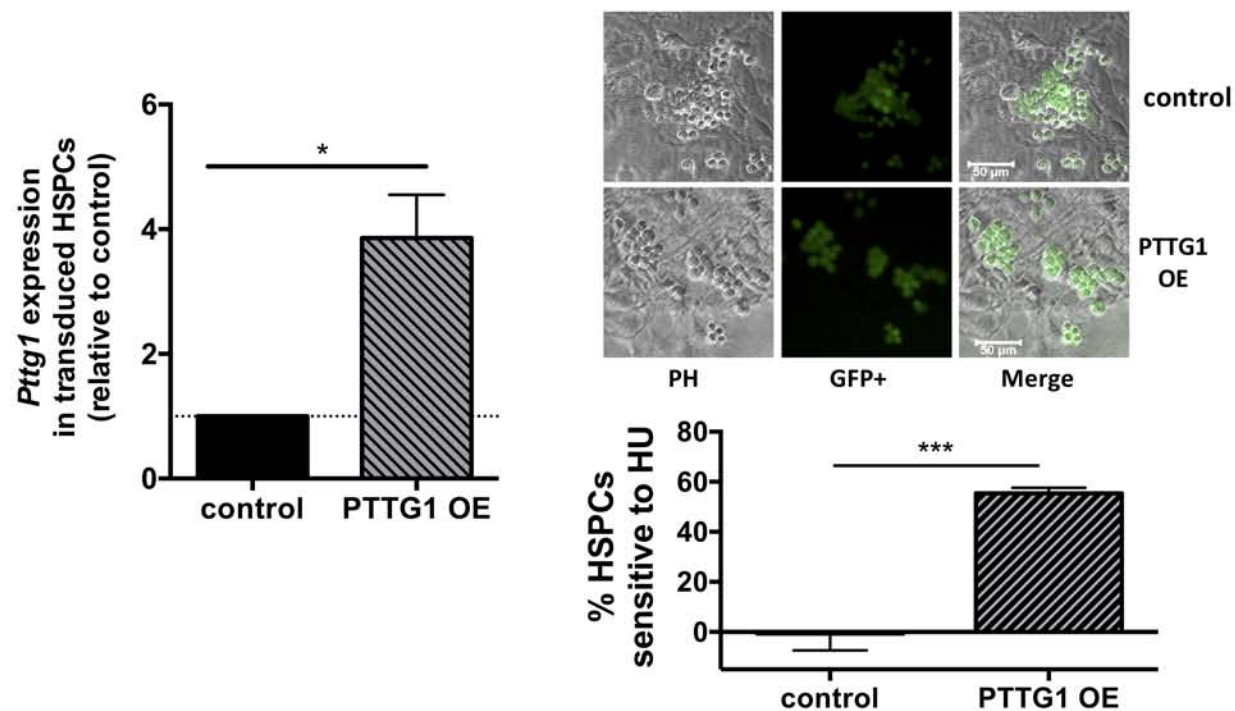
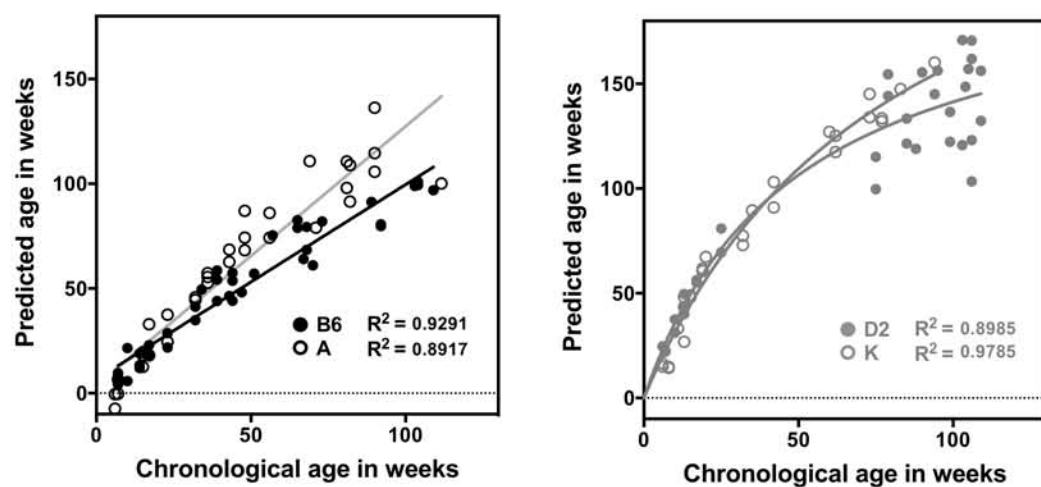
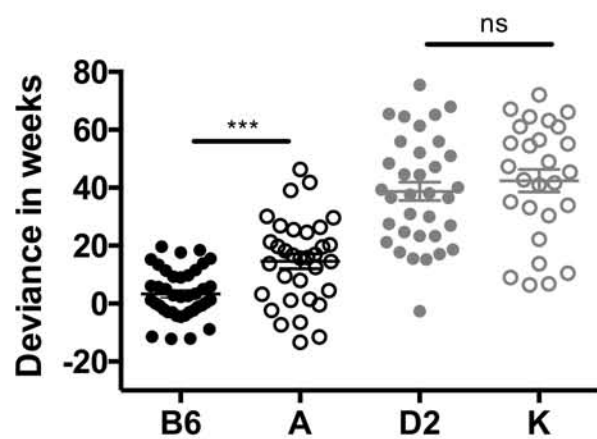
Fig 3**A****B****C****D****E**

Fig 4**A****B****C**

Supplementary data

Supplementary figure legends
Supplementary Tables on Excel files ONLY.

Suppl Fig 1: SNP analysis for B6, line A, D2 and line K mice from Fig 1D showing all chromosomes.

Suppl Fig 2: The chromosome 11 locus controls sensitivity of HSPCs to HU exposure but not HSPC frequency, cell cycle activity, apoptosis and replication fork stalling.

(A) LDBM cells from all four strains were treated with 200 $\mu\text{g/ml}$ HU or its solvent for 1 h and additionally with BrdU for the last 30 m. Thereafter, the number of LK cells which incorporated BrdU was measured by flow cytometry. Left panel: Representative FACS plots. Right panel: Quantification. $n=3$. (B) Total BM cells were isolated from the indicated mouse strains, treated with HU or its solvent following CAFC assay. At day 7 the cobblestone frequency of progenitors sensitive to HU treatment was measured. $n=4-5$. (C) Lin-cKit⁺ or Lin-cKit⁻ cells freshly isolated from B6 mice were plated in serial dilutions on FBMD-1 feeder layers. At day 7 and 14 cobblestones were counted and the frequency of cells to form colonies was calculated. $n=2$. (D) Telomere length in kMESF of HSPCs isolated from the four mouse strains. $n=3$. (E) HSPCs from all four mouse strains were treated with 200 $\mu\text{g/ml}$ HU or PBS for 1 h following analysis of *p16* expression by RT-PCR. $n=3$. (F) Total (left panel) or S-phase specific (right panel) AnnexinV⁺ rates of HSCs, LSKs and LK cells within the four mouse strains which were BrdU injected prior to analysis. $n=4$. (G) Upper panel: Schematic illustration of the experiment. LDBM cells from all four mouse strains were treated with either HU for 1 h or the corresponding solvent (PBS). Thereafter HU was removed and all samples were incubated for 15.5 h. Then the second sample was treated with HU whereas the third sample was treated with PBS. All samples were then treated with BrdU for 30 m following analysis of cell cycle

distribution and apoptosis. n=3. *P<0.05; **P<0.01; ***P<0.001; ****P<0.0001. BM = Bone marrow, HU = Hydroxyurea, LK = Lin-cKit+, LSKs = Lin-cKit+Sca1+ cells, HSCs = Hematopoietic stem cells, HSPCs = Hematopoietic stem and progenitor cell

Suppl Fig 3: Chromosome 11 associated *Pttg1* has an altered promotor sequence in D2/A mice leading to enhanced expression

(A) Upper panel: Schematic illustration of the *Pttg1* locus showing its exons, an 1,500 bp part of the corresponding promotor and all D2-specific SNPs. Lower panel: Comparison of the B6 and D2 transcriptional start regions as well as the predicted binding sites of transcription factors.

(B) Agarose gel electrophoresis comparing *Pttg1* promotor regions from our four mouse strains.

(C) Sequencing results showing the promotor and the region between the transcriptional and the ORF start of *Pttg1* within B6/K and D2/A. The asterisks indicate the 5' and 3' ends of the promotor fragments used for the luciferase assays. ORF = Opening reading frame

Suppl Fig 4: *Pttg1* promotes HU sensitivity of HSPCs

(A) PTTG1 *in silico* protein model showing B6- and D2-PTTG1. The arrow indicates the modest increase in 3₁₀ helices within the D2 variant. (B) GFP⁺ chimerism in peripheral blood of mice transplanted with cells expressing a control (*Egfp*) or *Pttg1-Egfp* 4 weeks post transplantation. 12-19 mice per group. (C) Representative FACS plots showing GFP⁺ cells (total LDBM cells vs LK cells) in BM 5 weeks after transplantation isolated from mice transplanted with lentiviruses mediating *Egfp* (control) or *Pttg1-Egfp* (PTTG1 OE) expression.

(D) Left panel: RT-PCR analysis of *Pttg1* upon knockdown in HSPCs from B6 mice. n=3. Right panel: HU sensitivity rates in HSPCs from D2 and line A mice upon knockdown of *Pttg1* and transplantation. n=3. Cells from line A and D2 mice (each 3 sets of mice) were used and transplanted into the corresponding B6 or D2 recipients. ***P<0.001; ****P<0.0001. HU =

Hydroxyurea, HSPC = Hematopoietic stem and progenitor cell, BM = Bone marrow, LDBM = Low density bone marrow, LK = Lin-cKit⁺ cells, OE = Overexpression

Suppl Table 1A:

% HU responses and mean life spans of all BXD and parental strains used for QTL mapping

Suppl Table 1B:

WebQTL analysis of the HU responses and mean life spans

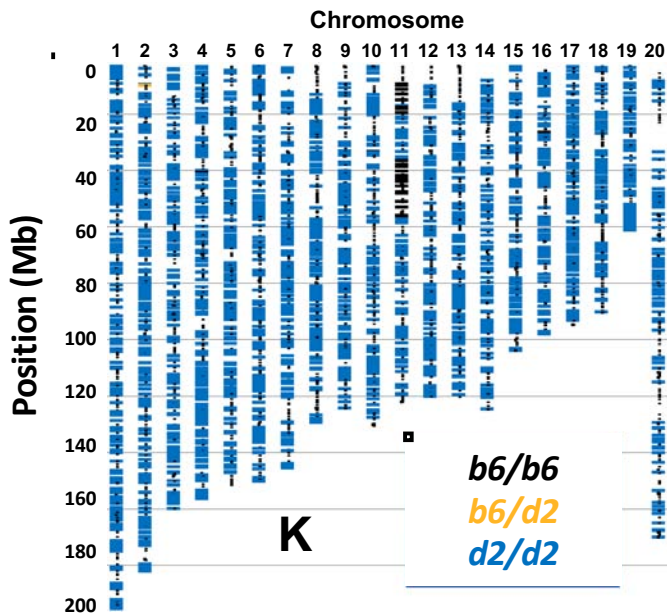
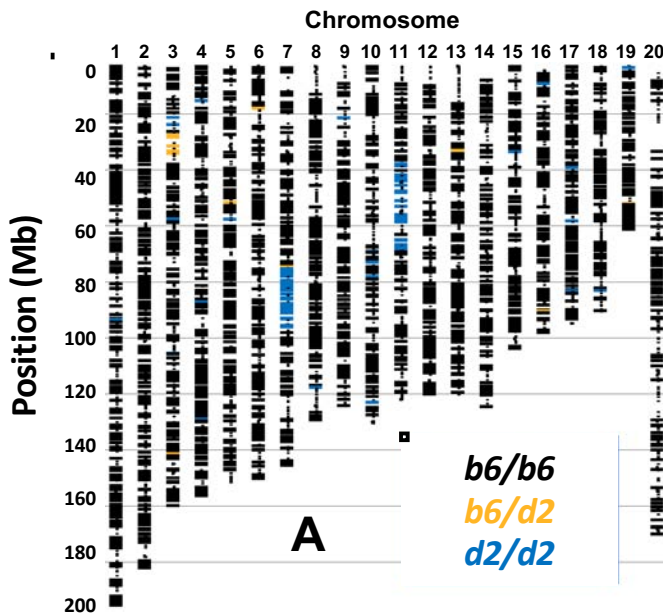
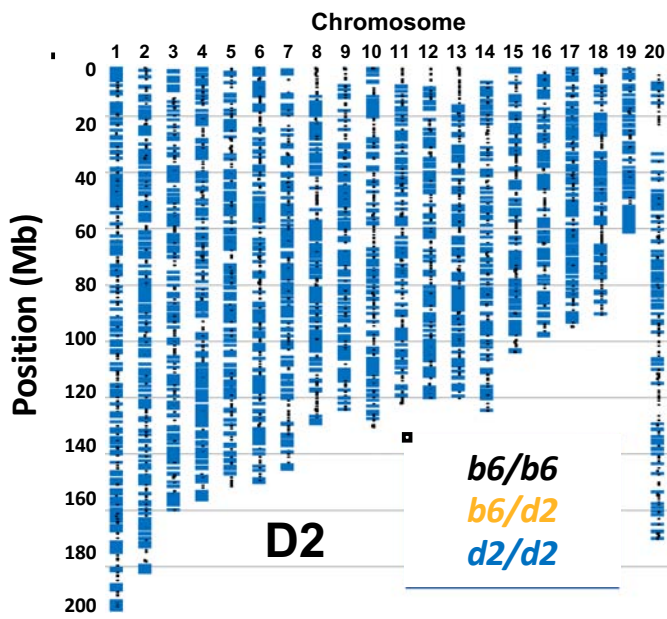
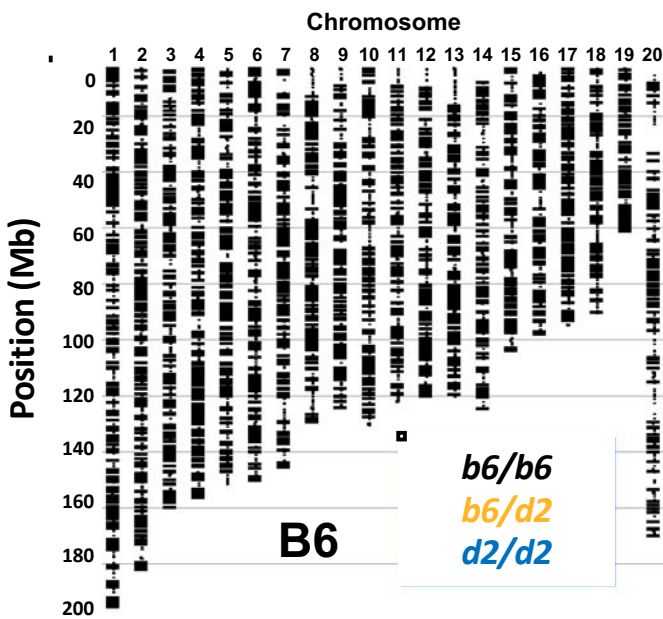
Suppl Table 2:

Complete list of SNP data for all analyzed strains. Indicated is the 18.6 Mb spanning region of chromosome 11.

Suppl Table 3:

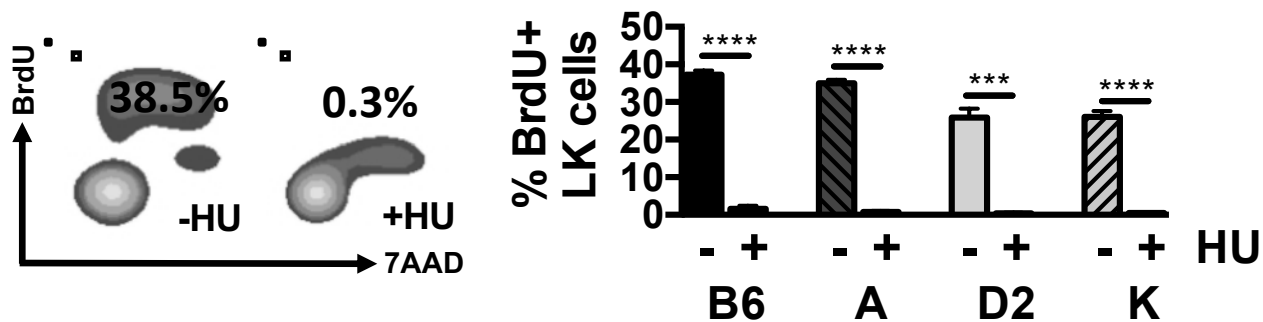
List of all 130 genes located on the proximal chromosome 11 locus. Indicated in brackets is the reading orientation.

Suppl Fig 1

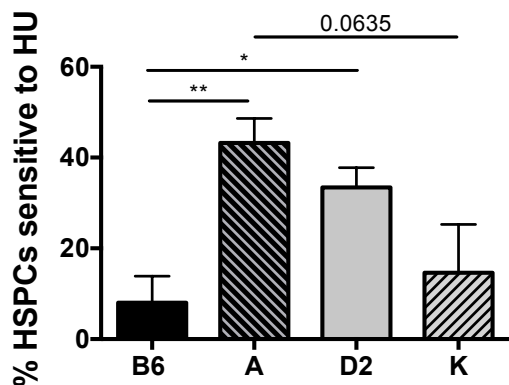


Suppl Fig 2

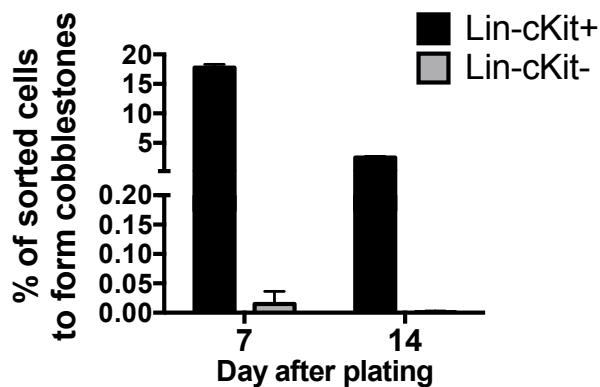
A



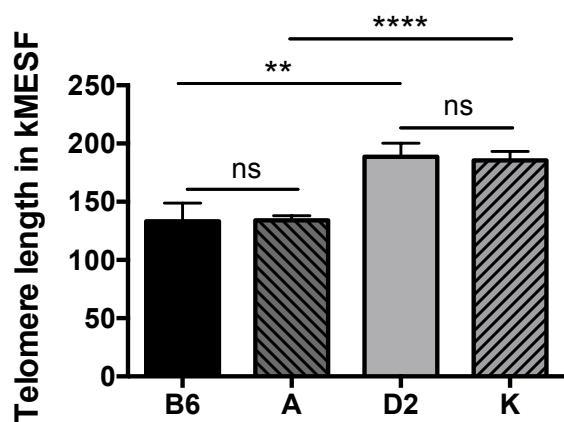
B



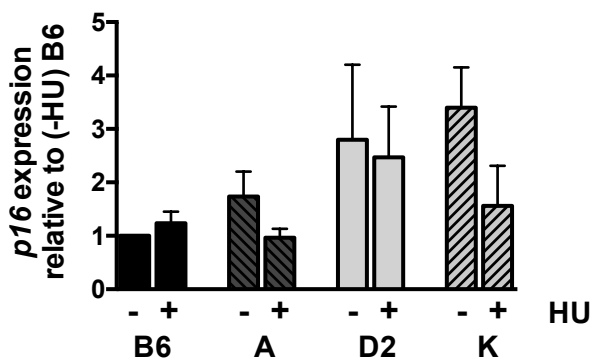
C



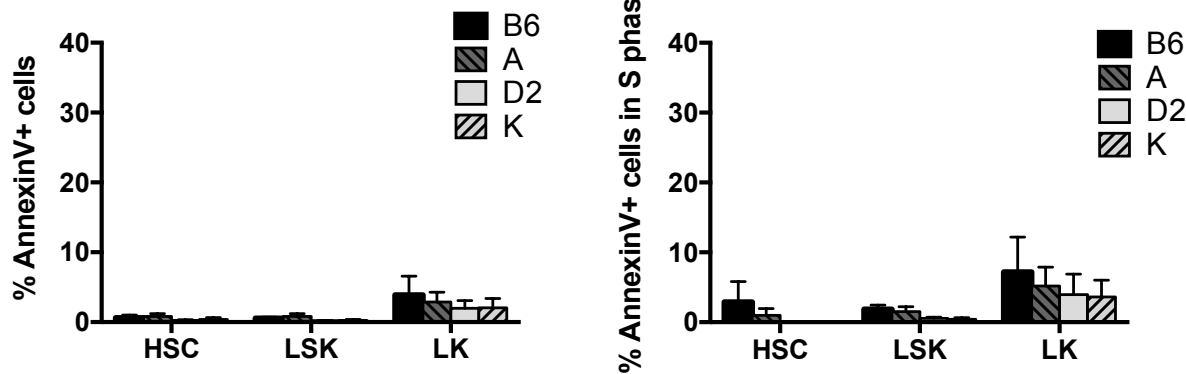
D



E

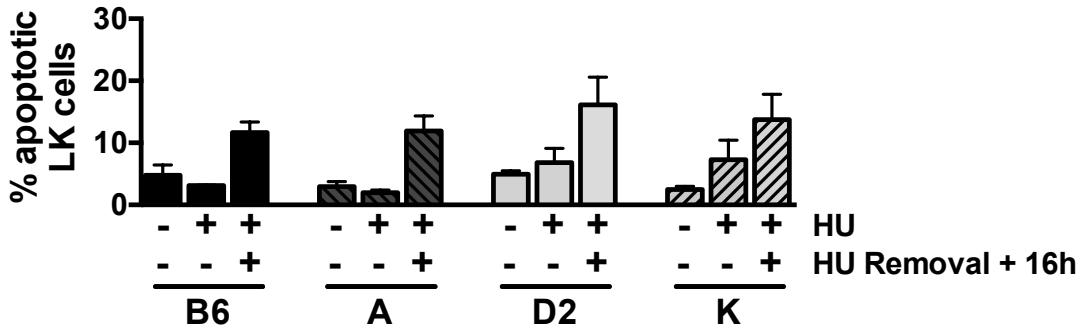
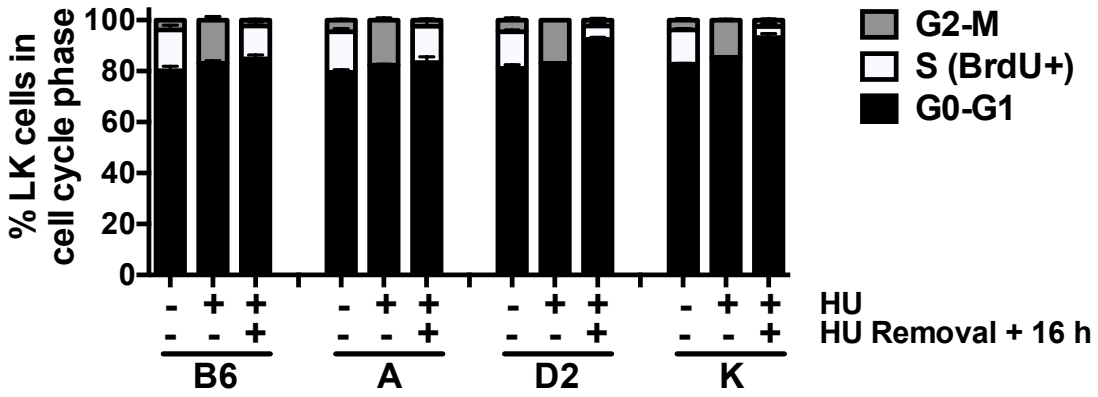
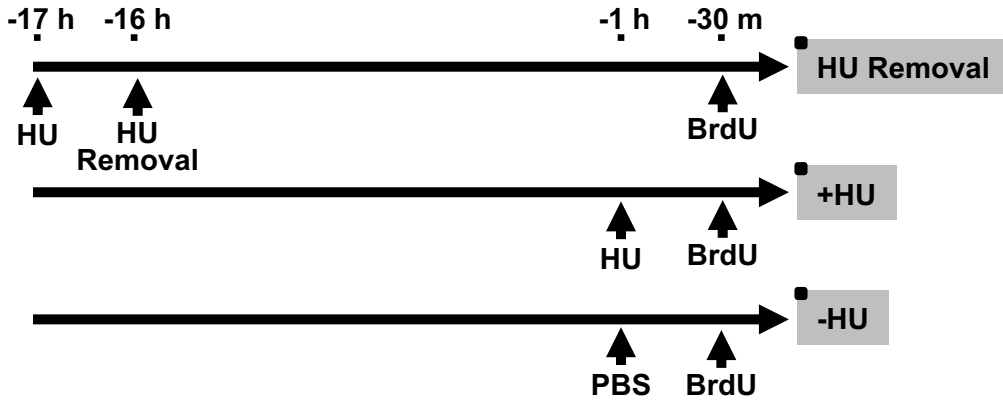


F



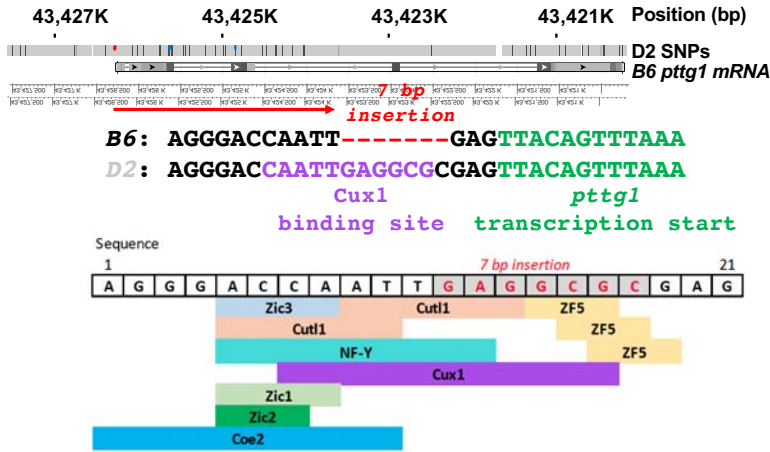
Suppl Fig 2 (Continued)

G

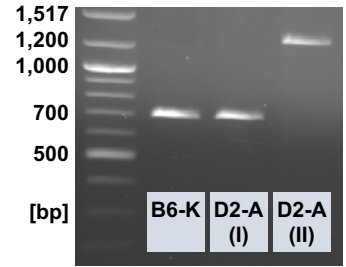


Suppl Fig 3

A



B



C

	ATACTTTGGAGACAGACGCGAGAGCTGGGCGGTGGCTGAAAACTTCCGTTGCCTCCATTGGTTCTCAGGCTGTAGGCCCCACCTCTCTCGGAGGGACCAATTGAG-----TTACAGTTTAACTGCG	
B6-K	* 10 20 30 40 50 60 70 80 90 100 110 120 130	
D2-A (I)	ATACTTTGGAGACAGACGCGAGAGCTGGGCGGTGGCTGAAAACTTCCGTTGCCTCCATTGGTTCTCAGGCTGTAGGCCCCACCTCTCTCGGAGGGACCAATTGAG-----TTACAGTTTAACTGCG	123
D2-A (II)	ATACTTTGGAGACAGACGCGAGAGCTGGGCGGTGGCTGAAAACTTCCGTTGCCTCCATTGGTTCTCAGGCTGTAGGCCCCACCTCTCTCGGAGGGACCAATTGAGGCCGAGTTACAGTTTAACTGCG	130
	GTGTGCCGGTCTGTGGTGGCGCAGTCTTCGGTGAAGTTAGCTGTGAGCTCGTCTGGGTGAGGCGCTCTTGGGCGAGCTTGGGTGGCGGGGAGGGCAGACCCGGGACTGGAGGTTGAAGCAGGGTCGG	
B6-K	140 150 160 170 180 190 200 210 220 230 240 250 260	
D2-A (I)	GTGTGCCGGTCTGTGGTGGCGCAGTCTTCGGTGAAGTTAGCTGTGAGCTCGTCTGGGTGAGGCGCTCTTGGGCGAGCTTGGGTGGCGGGGAGGGCAGACCCGGGACTGGAGGTTGAAGCAGGGTCGG	253
D2-A (II)	GTGTGCCGGTCTGTGGTGGCGCAGTCTTCGGTGAAGTTAGCTGTGAGCTCGTCTGGGTGAGGCGCTCTTGGGCGAGCTTGGGTGGCGGGGAGGGCAGACCCGGGACTGGAGGTTGAAGCAGGGTCGG	253
	GACGTGTGCTTCACTCGGCCCGGTCCCGAGGCGCTCTTGT-----	
B6-K	270 280 290 300 310 320 330 340 350 360 370 380 390	
D2-A (I)	GACGTGTGCTTCACTCGGCCCGGTCCCGAGGCGCTCTTGT-----	296
D2-A (II)	GACGTGTGCTTCACTCGGCCCGGTCCCGAGGCGCTCTTGT-----	296
	GGAATGGCTCCAACAGCTCAGGCTCTTTCCGTTAGTCTCACAAAGTGTCTTCTCTGGGTGGCGAGGCTGGCGCTTCACTGCACCCAGGTGCCCTTCTCTTTGGCTTCCTTTTCTCTTGGTCT	
B6-K	400 410 420 430 440 450 460 470 480 490 500 510 520	
D2-A (I)	-----	296
D2-A (II)	GGAATGGCTCCAACAGCTCAGGCTCTTTCCGTTAGTCTCACAAAGTGTCTTCTCTGGGTGGCGAGGCTGGCGCTTCACTGCACCCAGGTGCCCTTCTCTTTGGCTTCCTTTTCTCTTGGTCT	520
	CGTGCTCGACCCACA-----	
B6-K	530 540 550 560 570 580 590 600 610 620 630 640 650	
D2-A (I)	-----	311
D2-A (II)	TCTCCTTACCCGCTTCAAGAAAGTGTCTTGTCTTTTGTAGTGTGATGTCTCAATCGCACATTTGATCTCTTGGCAGAAATTTTCTTCTTGTGTGCTTCTTCAACCCGCTTCAAGAAAGTGTCT	311

B6-K	660 670 680 690 700 710 720 730 740 750 760 770 780	
D2-A (I)	-----	311
D2-A (II)	CTGCTCTTTGAGTGTGATGTCTCAATCGCACATTTGATCTCTTGGCAGAAATTTTCTTCTTGTGTGCTTCTTCAACCCGCTTCAAGAAAGTGTCT	780

B6-K	790 800 810 820 830 840 850 860 870 880 890 900 910	
D2-A (I)	-----	311
D2-A (II)	CGTGGTAGACTTATGGGCATTCCTTTTGAACAGTGCACATTTCCCTTGTATGTCTACAATATCACCTCTCTTGTAGATTGCGATGTATGTGGCCAAAGGAACAACGCCATGTTTCTTAAAGGCTCAGA	910

B6-K	920 930 940 950 960 970 980 990 1000 1010 1020 1030 1040	
D2-A (I)	-----	353
D2-A (II)	GAACATGTACGGGTGCCTTCTCTTTCCCTTTGTGTTCGTCAATTTTGGCAGTTACTGGAAGATGGTGGGCGGTCCAGCAACGCTGTTTTTACTTTTCTTCTTCCCTCCCTCCCACTTCAGGA	353

B6-K	1050 1060 1070 1080 1090 1100 1110 1120 1130 1140 1150 1160 1170	
D2-A (I)	-----	482
D2-A (II)	TCTCAAGCAGCCCTGGCTGGTCTTGAACCTTGT-ATGTAGCAGGAGGCCAAATTTGAGCATCTCTTGGCTTCTCTTTATAGCAGAGATTGTAGCTGGAGACAGTTTTGATGGGTGCCAACATAAAGT	482

B6-K	1180 1190 1200 1210 1220 1230 1240 * 1250 1260 1270 1280 1290 1300	
D2-A (I)	-----	612
D2-A (II)	ATTTCTGTAAGAGTGTAGTGTTTTATGACCTGGCGTGCAGATTTAGGATCTGGATTAAGCCTGTGACTTCCAGCTACTTATAAATTTTGTGCATAGTGCCTGGGTAAGCTTGGTCTCTGTTA	612

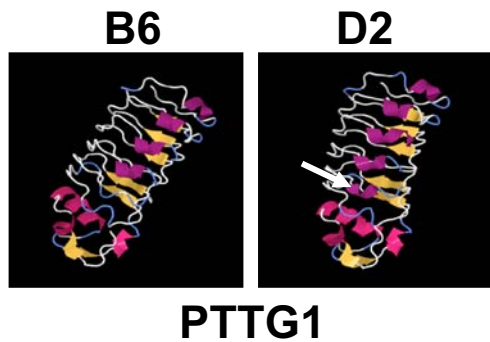
B6-K	1310 1320 1330 1340 1350 1360 1370 1380	
D2-A (I)	-----	696
D2-A (II)	CTGCGTAGTTTTTCCAGCCGCTCAATGCCAATATCTAATATTCAGGCTCTCCCTTAGAGTAATCCAGAATGGCTACTCTT	696

B6-K	1390 1400 1410 1420 1430 1440 1450 1460 1470 1480 1490 1500	
D2-A (I)	-----	1384
D2-A (II)	CTGCGTAGTTTTTCCAGCCGCTCAATGCCAATATCTAATATTCAGGCTCTCCCTTAGAGTAATCCAGAATGGCTACTCTT	1384

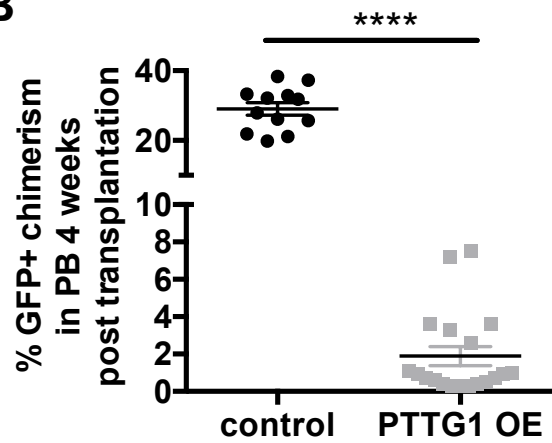
ORF Start

Suppl Fig 4

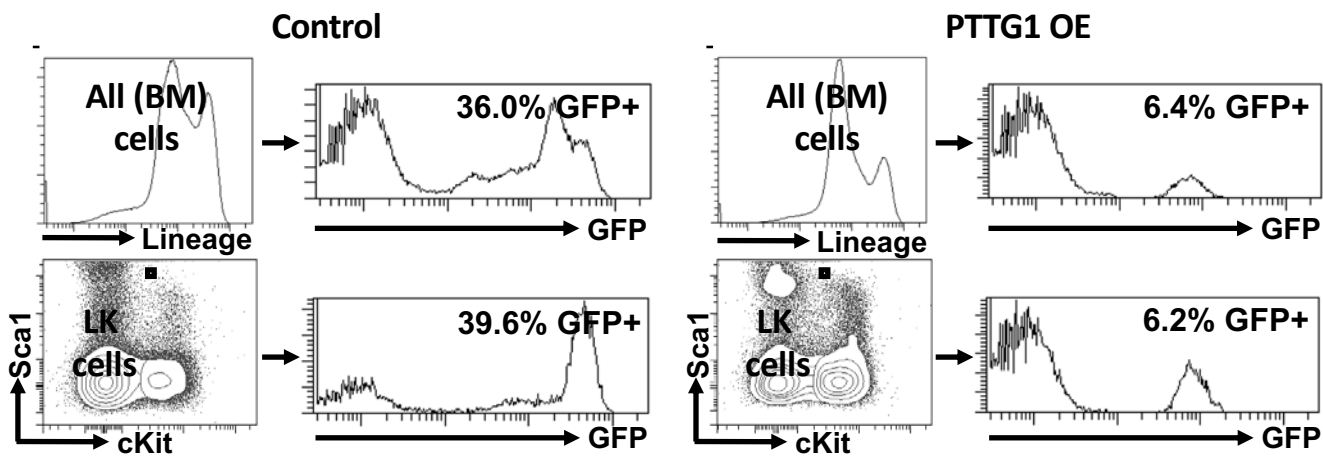
A



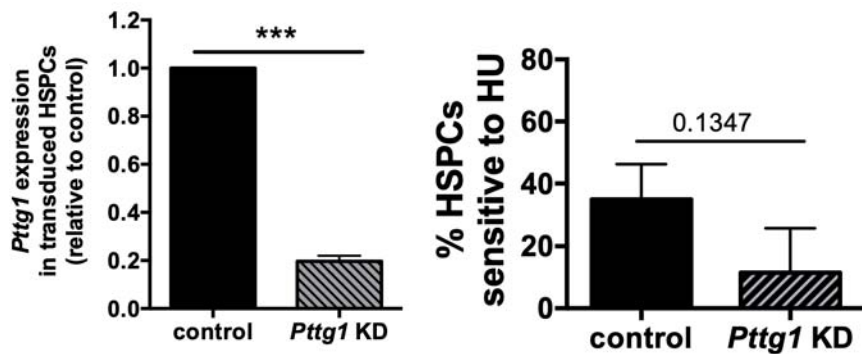
B



C



D



Supplementary methods

Genotyping of congenic mice

Congenic mice were generated as described in the main section. Offspring from line A was PCR analyzed with primers D11MIT177_F (GTAATGGTTATCACAGGAAGTTTGG) and D11MIT177_R (ACCCAGTCTGCAAACAT). The appearance of a 114 bp band indicated B6 mice congenic for the corresponding D2-locus, whereas a 124 bp band was B6-derived. Line K offspring was analyzed with primers D11MIT174_F (GGAAGGCATCCATGTTTGG) and D11MIT174_R (GGTAAGCCATTTGTAAACTGTGG). D2/B6 congenic mice corresponded to the appearance of a band at 147 bp, whereas non-congenic mice showed a band at 165 bp.

Cell culture

NIH/3T3 mouse fibroblasts (ATCC) were cultured in DMEM and HEK-293 cells (ATCC) in IMDM (ThermoFisher) supplemented with 10% FBS and antibiotics (#P11-010, ThermoFisher) at 37 °C and 5 % CO₂. FBMD-1 cells were kindly gifted by José Cancelas and cultured at 33 °C and 5 % CO₂ in IMDM containing L-glutamine (1/100 GlutaMAX, Gibco), 5% horse serum (Sigma Aldrich), 10% fetal bovine serum (sera from Gibco), 10⁻⁴ mol/L β-mercaptoethanol, 10⁻⁵ mol/L hydrocortisone (Sigma, St Louis, MO), 80 U/mL penicillin and 80 µg/mL streptomycin (both from Gibco). BM or LDBM cells were incubated in IMDM with 10% FBS and antibiotics.

Cell cycle and apoptosis staining

Mice were injected i.p. with 200 µl 2.5 mg/ml BrdU (#559619, BD Pharmigen) for 45 m prior to analysis. For apoptosis and cell-cycle analyses, 2*10⁶ LDBM cells were stained with a cocktail of biotinylated lineage antibodies (CD5, B220, Mac-1, CD8a, Gr-1, Ter-119, BD) after Fc block (#553142, BD) for 15 m. Cells were washed once and stained with the following

antibodies from eBioscience: Streptavidin APC-Cy7, anti-c-Kit-Alexa 700 (clone ACK2), anti-CD34 APC (RAM34), and anti-Sca1 PE-Cy7 (D7) for 1 h on ice. For identification of apoptotic cells, the antibody stained cells were washed and incubated in Annexin V Binding Buffer (#556454, BD) containing Annexin V (#560506, BD) for 20 m at RT and analyzed by flow cytometry. For cell cycle analysis, antibody stained cells were fixed and permeabilized using Cytotfix/Cytoperm buffer (#554722, BD). Cells were again permeabilized the next day using Cytotfix Buffer Plus (#561651, BD) and Cytotfix/Cytoperm buffer (BD). Cells were then treated with 30 $\mu\text{g}/\mu\text{l}$ DNase (#D4513, Sigma Aldrich) in PBS with $\text{Ca}^{2+}/\text{Mg}^{2+}$ for 1.5 h at 37 °C and after washing incubated with anti-BrdU antibody (#559619, BD) for 20 m at RT. Directly before analysis with a LSRII flow cytometer (BD), cells were resuspended in PBS and 7AAD (#559925, BD) was added. HSCs were defined as Lin-cKit+Sca-1+CD34-, LSK represented Lin-cKit+Sca1+cells, and hematopoietic progenitor cells were gated Lin-cKit+Sca1-. The data acquisition and analysis were performed using BD FACS DIVA.

Plasmids and cloning of Pttg1

Expression vector SF-LV-cDNA-EGFP and packaging plasmids pMD2.G/pxPAX2 as described previously were kindly provided by Lenhard Rudolph.^{1,2} Murine *Pttg1* ORF was PCR-cloned from a B6 cDNA library and transferred into SF-LV-cDNA-EGFP vector with *XhoI* and *NotI* using the following primers:

5'XHOI_MPTTG1: ATAATCTCGAGATGGCTACTCTTATCTTTG

3'NOTI_MPTTG1: GATATGCGGCCGCTTAAATATCTGCATCGTAACAA

Cloning success was confirmed by restriction analysis and DNA sequencing.

Generation of lentiviral particles

Lentiviruses were generated with the calcium phosphate transfection method as described previously³ with HEK-293 cells (#632180, Clontech) using the Calphos Mammalian

Transfection Kit (#062013, Clontech). The absolute ratio of SF-LV-cDNA-EGFP or shRNA pGFP-C-shLenti, pxPAX2 and pMD2.G was 3:2:1. After 24 h and 48 h, raw viral supernatants were harvested, filtered (0.45 μ m), and concentrated for 2 h with 25 000 rpm at 4 °C. Infectious titers were determined on NIH/3T3 or 293T cells performing titration. Multiplicity of infection (MOI) of 1 was set when 50 % of NIH/3T3 cells are GFP+. For generation of *Pttg1* knockdown particles, PTTG1 Mouse shRNA pGFP-C-shLenti (#TL502795, OriGene Technologies) was used.

Transduction and transplantation

Lin⁻ cells isolated from B6 mice as described⁴ were seeded on Retronectin (Takara, Japan) coated 24 well plates using IMDM supplemented with 100 ng/ml mG-CSF, mTPO and mSCF (Prospec). After 24 h cells were transduced for 6-8 h with lentiviruses coding for *Egfp* (control), *Pttg1-Egfp* or *Pttg1*-shLenti using a MOI of 15-25. The next day cells were harvested with Cell Dissociation Reagent (#07174, STEMCELL Technologies), washed, resuspended in PBS and transplanted. For transplantation between 2.0 and 5.0*10⁵ B6 Lin⁻ cells were tail-injected into lethally irradiated (7+4 Gy) B6 or D2 recipient mice. After 4 weeks, GFP⁺ chimerism in peripheral blood was analyzed using anti-CD3e (clone 145-2C11), anti-B220 (clone RA3-6B2), anti-Mac-1 (clone M1/70) and anti-Gr-1 (clone RC57BL/6-8C5) antibodies from eBioscience. 5-6 weeks after transplantation mice were sacrificed and GFP⁺/APC⁻ cells were sorted using a BD Aria II/III device.

RT-PCR

Total RNA was extracted from cells using the Qiagen Micro RNA Kit and cDNA was synthesized using 500 ng of total RNA and the QuantiTect Reverse Transcription Kit (#205310, Qiagen) according to the supplier's protocols. Briefly, 2 μ l of gDNA Wipeout buffer and 500 ng of total RNA were added to the reaction system which was adjusted to a volume of 14 μ l

using RNase-free water and incubated at 42 °C for 2 m. Next, 4 µl 5X Quantiscript Reverse Transcriptase Buffer, 1 µl Quantiscript Reverse Transcriptase and 1 µl dNTP mixture were added to the reaction system and incubated at 42 °C for 15-30 m and then at 95 °C for 3 m. Quantitative PCR (qRT-PCR) was performed using specific primers targeted against *Pttg1*, *p16* and *Gapdh* from Thermo Fisher Scientific (Mm00479224_m1, Mm00494449_m1, Mm99999915_g1). For PCR amplification, we took 2 µl of cDNA, 10 µl 2x TaqMan Universal PCR Master Mix (#4304437, Thermo Fisher Scientific), 1 µl TaqMan primer and added RNase-free water to a total volume of 20 µl. Using a ABI Prism 7900HT device (Applied Biosystems), the reaction was as follows: Initial heating step by 95 °C for 10 m, followed by 40 cycles of two-step reactions at 95 °C for 15 s and 60 °C for 1 m. Analysis was done with SDS 2.4 and RQ Manager 1.2.1 (Applied Biosystems).

Immunofluorescence imaging

Sorted cells were treated as indicated. Thereafter, cells were harvested and fixed using Cytifix solution (#554655, BD) for 20 m at 4 °C. Following a 20 m permeabilization step in PBS + 0.2% Triton X, cells were blocked for 20 m in PBS containing 10% donkey serum (D9663, Sigma Aldrich). Primary antibody was anti-γH2AX (#05-636, Millipore) at 1:1000. Following an incubation step for 1 h at 37 °C, cells were washed twice and incubated using secondary antibodies (anti-mouse Alexa488, Jackson ImmunoResearch) at a dilution of 1:1,000. Before analyzing cells were mounted on glass slides using Antifade with DAPI solution (#P-36931, ThermoFisher). Cells were analyzed using a Zeiss Observer Z.1 microscope. Pictures were taken with a Zeiss LSM 710 laser scanning microscope.

Western Blot

5*10⁶ LDBM cells were resuspended and incubated for 10 m at 95 °C in 1xSDS sample buffer containing 10 % SDS (Carl Roth), 10 mM β-mercaptoethanol (Carl Roth), 0,2 M Tris-HCl pH

6.8 (Biorad) and 0.05 % bromophenol blue (Sigma) and sonicated for 5 m. Equal amounts of protein were loaded onto a 12 % polyacrylamide gel. After running the gel first 10 m at 95 V and then 80 m at 110 V, the gel was blotted onto a nitrocellulose blotting membrane (Amersham Protran 0,45 µm, GE Healthcare Life Sciences) using a Trans-Blot SD semi-dry Transfer Cell (Biorad). Proteins were visualized by overnight incubation with rabbit-anti-PTTG1 antibody (#ABIN484400, Assay BioTech) and mouse-anti-β-actin (1:1000) antibody (#A1978, Sigma Aldrich) after blocking with PBS containing 5 % milk powder. After washing, the membranes were incubated with rabbit-IgG-HRP or mouse-IgG-HRP antibody (#sc-2077, #sc-2314, Santa Cruz) for 1 h. For detection ECL-reagent from the Super Signal West Femto Kit (#34094, Thermo Scientific) was used.

Flow-FISH

Analysis of telomere length by flow cytometry (Flow-FISH) was performed as described^{5,6} using 10⁴ LK cells. Samples were measured on a BD LSR II.

DNA sequencing

Fragments of various sizes with respect to the PTTG1 promotor regions of B6, line A, D2 and line K mice were amplified from the corresponding genomic DNA by PCR with Herculase II (#600675, Agilent) according to their instructions, separated by gel electrophoresis, purified, digested with NheI-HF/EcoRV-HF (#R3131, #R3195, New England Biolabs) and cloned into digested/dephosphorylated pNL1.1[Nluc], #N1001, Promega) using T4 DNA ligase (#M0202S, New England Biolabs), XL1-Blue competent cells (#200249, Agilent) and the QIAprep Spin Miniprep Kit (#27106, Qiagen). Plasmids were sent to GATC Biotech (Konstanz, Germany) for sequencing. Analysis and alignments were done with Lasergene DNASTar.

Cloning primers:

5'NheI-B6/D2_PTTG1_pr1: ATTAGCTAGCATACTTTGGAGACAGACGCGAG

3'EcoRV-B6/D2_PTTG1_pr2: ATAAGATATCCCAGGGCTGCTTGAGATCCT
3'EcoRV-B6/D2_PTTG1_pr3: AAGCGATATCTGGAGAAGTCAACAGGCTTAATCC
5'NheI-B6/D2_PTTG1_pr4: ATTAGCTAGCGAAGCCAAAACCATAAAAGTGAGC
3'EcoRV-B6/D2_PTTG1_pr5: ATAAGATATCCCCGGGCTGCTTGAGATCC
3'EcoRV-B6/D2_PTTG1_ORF: ATAAGATATCAAGAGTAGCCATTCTGGATTACTC

Sequencing primers:

PNL1[NLUC]_SEQ_FOR: GTGTGAATCGATAGTACTAA
PNL1[NLUC]_SEQ_REV: AAGGACTTGGTCCAGGTTGT

Analysis of SNPs and the pttg1 promotor

The image in *Suppl Fig 3A* showing SNPs in D2 and B6 regions of *Pttg1* was generated using the JAX/MCI database (<http://www.informatics.jax.org/snp>). Alignment of D2- and B6 promotor regions was done with Lasergene DNASTar. Transcription factor binding site prediction was performed with PROMO:

http://algggen.lsi.upc.es/cgi-bin/promo_v3/promo/promoinit.cgi?dirDB=TF_8.3

3D in silico modelling

Models of B6- and B2-PTTG1 (primary sequences see below, differences are highlighted) were generated using Jmol:

<http://jmol.sourceforge.net/index.en.html>

B6-PTTG1

MATLIFVDKDNEEPGRRLASKDGLKLGTVKALDGLQVSTPRVGKVFNAPAVPKA
SRKALGTVNRVAEKPMKTGKPLQPKQPTLTGKKITEKSTKTQSSVPAPDDAYPEIEKF
FPFNPLDFESFDLPEEHQISLLPLNGVPLMTLNEERGLEKLLHLGPPSPLKTPFLSWESD
PLYSPPSALSTLDVELPPVCYDADI

D2-PTTG1

MATLIFVDKDNEEPG**S**R**L**ASKDGLKLG**S**GVKALDGKLVSTPRVGKVFNAPAL**L**PKA
SRKALGTVNRVAEKPMKTGKPLQPKQPTLTGKKITEKSTKTQSSVPAPDDAYPEIEKF
FPFNPLDFESFDLPEEHQISLLPLNGVPLMTLNEERGLEKLLHLGPPSPLKTPFLSWESD
PLYSPPSALSTLDVELPPVCYDADI

Luciferase Assay

B6/K and D2/A promotor regions were cloned as described under the *DNA sequencing section* using 5'NheI-B6/D2_PTTG1_pr1 and 3'EcoRV-B6/D2_PTTG1_pr3. Cloning success was confirmed by restriction analysis and DNA sequencing.

The day before analysis, 30,000 NIH/3T3 cells were seeded onto cell-culture coated 24 well plates (Sarstedt) using IMDM medium with FCS and antibiotics. The next day, medium was removed and 400 µl fresh medium without antibiotics was added. 4 h later, each sample was transfected for 18 h with FuGene 6 transfection reagent (#E2693, Promega) according to their manual using 96 µl OPTI-MEM (#31985-062, Gibco), 1.5 µl FuGene 6 reagent, 100 ng Salmon Sperm DNA (#15632-011, Invitrogen), 75 ng pGL4.54 plasmid (#KM359769, Promega), which codes for the firefly luciferase and 75 ng of the pNL1.1 vectors coding for the various promotor fragments and the Nanoluc luciferase. Assay was done with the Dual-Luciferase Reporter Assay System (#E1910, Promega) in three rounds and triplicates according to the manufacturer's protocol and included a positive (pNL1.1CMV[Nluc/CMV], #N1091, Promega) and a negative (pNL1.1[Nluc], #N1001, Promega) control. For detection of chemiluminescence Nunclon Delta Surface plates (#136101, Thermo Scientific) and a GloMax 96 Microplate Luminometer (#E4861, Promega) were used. The relative luminescence was calculated by dividing the measured Nanoluc luminescence with the Firefly luminescence values.

Supplementary references

1. Wang J, Sun Q, Morita Y, et al. A differentiation checkpoint limits hematopoietic stem cell self-renewal in response to DNA damage. *Cell*. 2012;148(5):1001-1014.
2. Cribbs AP, Kennedy A, Gregory B, Brennan FM. Simplified production and concentration of lentiviral vectors to achieve high transduction in primary human T cells. *BMC Biotechnol*. 2013;13:98.
3. Moehrle BM, Nattamai K, Brown A, et al. Stem Cell-Specific Mechanisms Ensure Genomic Fidelity within HSCs and upon Aging of HSCs. *Cell Rep*. 2015;13(11):2412-2424.
4. Brown A, Pospiech J, Eiwien K, et al. The Spindle Assembly Checkpoint Is Required for Hematopoietic Progenitor Cell Engraftment. *Stem Cell Reports* 2017;9(5):1359–1368.
5. Rudolph KL, Chang S, Lee HW, et al. Longevity, stress response, and cancer in aging telomerase-deficient mice. *Cell*. 1999;96(5):701-712.
6. Hultdin M, Grönlund E, Norrback K, Eriksson-lindström E, Just T, Roos G. Telomere analysis by fluorescence in situ hybridization and flow cytometry. *Nucleic Acids Res*. 1998;26(16):3651-3656.